Article

Effect of Phenolic Compounds on the Synthesis of Gold Nanoparticles and Its Catalytic Activity in the Reduction of Nitro Compounds

Elisabete C. B. A. Alegria [1,2,*] [ID]**, Ana P. C. Ribeiro** [1,*] [ID]**, Marta Mendes** [1,2]**, Ana M. Ferraria** [3] [ID]**, Ana M. Botelho do Rego** [3] [ID] **and Armando J. L. Pombeiro** [1,*]

[1] Centro de Química Estrutural, Instituto Superior Técnico, Universidade de Lisboa, Av. Rovisco Pais, 1049-001 Lisboa, Portugal; marta.s.mendes@hotmail.com

[2] Chemical Engineering Departament, ISEL-Instituto Superior de Engenharia de Lisboa, Instituto Politécnico de Lisboa, 1959-007 Lisboa, Portugal

[3] CQFM-Centro de Química-Física Molecular and IN-Institute for Nanosciences and Nanotechnologies and IBB-Institute for Bioengineering and Biosciences, Instituto Superior Técnico, Universidade de Lisboa, 1049-001 Lisboa, Portugal; ana.ferraria@tecnico.ulisboa.pt (A.M.F.); amrego@tecnico.ulisboa.pt (A.M.B.d.R.)

[*] Correspondence: ebastos@deq.isel.ipl.pt (E.C.B.A.A.); apribeiro@tecnico.ulisboa.pt (A.P.C.R.); pombeiro@tecnico.ulisboa.pt (A.J.L.P.)

check for updates

Abstract: Gold nanoparticles (AuNPs) were prepared using an eco-friendly approach in a single step by reduction of $HAuCl_4$ with polyphenols from tea extracts, which act as both reducing and capping agents. The obtained AuNPs were characterized by scanning electron microscopy (SEM), transmission electron microscopy (TEM), ultraviolet–visible spectroscopy (UV–vis), and X-ray photoelectron spectroscopy (XPS). They act as highly efficient catalysts in the reduction of various aromatic nitro compounds in aqueous solution. The effects of a variety of factors (e.g., reaction time, type and amount of reducing agent, shape, size, or amount of AuNPs) were studied towards the optimization of the processes. The total polyphenol content (TPC) was determined before and after the catalytic reaction and the results are discussed in terms of the tea extract percentage, the size of the AuNPs, and their catalytic activity. The reusability of the AuNP catalyst in the reduction of 4-nitrophenol was also tested. The reactions follow pseudo first-order kinetics.

Keywords: gold nanoparticles; phytochemicals; catalysis; reduction; nitro compounds

1. Introduction

Metallic nanoparticles (NPs) are often synthesized using chemical methodologies involving organic and inorganic reducing agents, which can also act as stabilizing agents to avoid the coalescence of the NPs, such as hydrazine, sodium borohydride ($NaBH_4$), or *N*,*N*-dimethylformamide [1].

The environmental risks and toxicity associated with these chemicals have led to a growing interest in environmentally friendly and sustainable methods for the synthesis of a variety of metallic NPs with specific sizes and aggregations [2]. Some of these new "green" synthetic processes concern microorganisms, such as bacteria [3,4] or fungi [5], and plant extracts [6–12].

The use of phytochemicals in the synthesis of NPs, which include leaves, fruits, seeds, and stems, is starting to be developed and presents some advantages over the application of microorganisms in view of the high diversity of plant extracts and the simplicity and low cost of the method [2,6–10].

Gold nanoparticles (AuNPs) are recently gaining a great interest due to their potential application in many fields, such as catalysis, biosensing, photonics, drug-delivery systems, and antimicrobial agents [13–19]. They also have been used to catalyze electron-transfer and oxidation reactions,

specifically glucose oxidation [20], aerobic alcohol oxidation [21], reduction of nitroarenes in aqueous media [22], or CO oxidation and propylene epoxidation [23]. AuNPs produced from vegetable oil in a green reaction medium have also been used in antimicrobial paints [24].

Due to its health benefits and antioxidant properties, the use of black tea [7] for the production of biocompatible AuNPs is being tested in diverse areas such as health and energy. The phytochemicals present in tea show a dual role: as reducing agents to reduce gold and as stabilizers to provide a robust coating on the AuNPs in a one-pot process.

In this work, we used a black tea extract to act as a low-cost reducing and stabilizing agent for AuNPs synthesis, determined the variation of the total polyphenol content (TPC) and the atomic concentration of each element detected by XPS after the AuNPs were produced, and explored the catalytic properties of the AuNPs synthesized via tea extract solutions in simple model reactions; that is, the reduction of various nitro compounds (2- and 4-nitrophenol; 2-, 3-, and 4-nitroaniline, or nitrobenzene) in aqueous solution.

In particular, the reduction of 4-nitrophenol has become the model reaction for the evaluation of the catalytic activity of metallic NPs, namely with Ag [25,26], Au [27–32], or Pd [33] metals. The existence of a well-defined absorption band characteristic of this substrate allows to easy screening of the reaction by UV–vis spectroscopy [34–36].

2. Materials and Methods

2.1. Reagents and Instrumentation

All synthetic work was performed in air. The reagents and solvents were obtained from commercial sources and used without further purification or drying. Black tea from Tetley (Yorkshire, UK); 4-nitrophenol (4-NP) (Acros Organics, Morris Plains, NJ, USA); 2-nitrophenol (2-NP) (BDH, St. Louis, MO, USA); nitrobenzene (NB) (Acros); 4-aminophenol (4-AP) (Aldrich, St. Louis, MO, USA); 2-aminophenol (2-AP) (BDH); 2-, 3-, and 4-nitroaniline (2-, 3-, and 4-NA) (Fluka, Bucharest, Romania); 2-, 3-, and 4-phenylenediamine (2-, 3-, and 4-PD) (Fluka, Bucharest, Romania); $NaBH_4$ (Acros Organics, Morris Plains, NJ, USA); ascorbic acid (Merck, Darmstadt, Germany); D-glucose (Aldrich, St. Louis, MO, USA); NH_4Cl (Panreac, Barcelona, Spain); N_2H_4 (Aldrich, Missouri, USA); and tetrachloroauric(III) acid ($HAuCl_4 \cdot 3H_2O$) (99.99%, Aldrich, St. Louis, MO, USA) were used as received.

The synthesized AuNPs using tea extracts were characterized using UV–vis, XPS, XRD, SEM, EDS, and TEM techniques. UV–visible spectroscopic measurements of the synthesized AuNPs were carried out on a PerkinElmer (Massachusetts, EUA) Lambda 750 UV–visible spectrophotometer. XPS analysis was performed by a XSAM800 spectrometer from KRATOS, Manchester, UK. Details on operation conditions, data acquisition, and treatment were published elsewhere [37], except for the energy reference used to correct the charge shift which was the binding energy of aromatic carbons centered at 284.7 eV. TEM measurements were performed on a transmission electron microscope Hitachi 8100 (Tokyo, Japan) with ThermoNoran light elements EDS detector and digital image acquisition. Morphology and distribution of AuNPs were characterized using a scanning electron microscope (SEM) (JEOL 7001F with Oxford light elements EDS detector and EBSD detector). FTIR (Fourier transform) measurements were carried out on a Bruker Vertex 40 Raman/IR spectrometer (Massachusetts, EUA) in a range from 4000 to 100 cm^{-1}.

2.2. Preparation of Au Nanoparticles Using Tea Extracts

The preparation of AuNPs using tea extracts followed the method described previously [15]. The tea solutions were prepared by mixing a weighted amount of dried black tea leaves (2 g) with 100 mL of distilled water followed by vigorous stirring for 15 min at room temperature in order to obtain three solutions with different percentages of tea (1, 5, or 10% *w/v*). After filtration, 6 mL of each tea solution was transferred to a glass vial and to each of them 0.1 mL of a tetrachloroauric

acid ($HAuCl_4 \cdot 3H_2O$) solution (0.1 M) was added, with stirring for 20 min at room temperature. The solution changed from pale yellow to red color almost instantaneously, indicating the formation of Au nanoparticles. UV–vis spectroscopy was used to confirm the successful formation of the AuNPs on account of the occurrence of the characteristic surface plasmon resonance (SPR) band of AuNPs (538 nm) in the visible region [22,38–40]. X-ray photoelectron spectroscopy analysis confirms the existence of gold and its metallic state in the AuNPs for the 1% tea extract.

2.3. Determination of Total Polyphenol Content in Tea by the Folin–Ciocalteu Method

The total polyphenol content (TPC) was determined colorimetrically using the Folin–Ciocalteu phenol reagent and gallic acid as the calibration standard following the reported method [41]. The absorbance of the various reducing media was measured by a UV–vis spectrophotometer at a wavelength of 765 nm, and a calibration curve was constructed with 10 gallic acid standard solutions (12.5–500 mg/L; R^2 = 0.9996).

2.4. Reduction of Nitro Compounds in Aqueous Solution

All catalytic reactions were performed in a standard 3 mL quartz cuvette with a 1 cm path length. Stock aqueous solutions of 4-nitrophenol (0.012 M) and $NaBH_4$ (0.1 M) were freshly prepared for each experiment to minimize hydrolysis. Stock aqueous solutions of 2.5 mL of water and 0.5 mL AuNP tea solution (1, 5, or 10%) were prepared. In standard conditions, 0.5 mL of the diluted AuNP solution is placed in the cuvette and 2.5 mL of distilled water is added. To this solution, 100 µL of the nitro compound (2- or 4-nitrophenol; 2-, 3-, or 4-nitroaniline; or nitrobenzene) and finally 50 µL $NaBH_4$ solution (0.1 M) was added. The UV–vis absorbance spectra were recorded in the 200–700 nm range at 2 min intervals. The catalytic activity was quantified in terms of conversion of the substrate and turnover frequency (TOF), considering that 2- or 4-aminophenol; 2-, 3-, or 4-phenylenediamine; and aniline are the only reduction products.

3. Results and Discussion

3.1. Au Nanoparticle Identification

The addition of $HAuCl_4 \cdot 3H_2O$ to a black tea extract resulted in an almost instantaneous change of color from light yellow to red, which indicates [22,38–40] the effectiveness of the Au reduction. As expected, the obtained Au colloid solution exhibits in the UV–vis spectrum the typical [22,38–40] absorption band due to the presence of Au nanoparticles (AuNPs), without any significant shift or change in the intensity over time.

The effect of different concentrations of tea extract (1, 5, and 10% *w/v*) solutions on the size and dispersity of the AuNPs was analyzed (onwards, the AuNPs solutions will be named as AuNPs 1% tea, AuNPs 5% tea, and AuNPs 10% tea, respectively). Using different concentrations of tea extract (1, 5, and 10%) enables the variation of the size of the produced nanoparticles and as a result, the colors of their dispersion (Figure 1 and Figure S1).

The surface plasmon resonance (SPR) bandwidth for AuNPs 1, 5, and 10% tea follows the predicted behavior, as it increases with the increasing size of gold nanoparticles [42–44]. In fact, the shorter bandwidth for the AuNPs 1% tea solution at 538 nm confirms the smaller size of these NPs (8–24 nm diameter range, see below), relative to the absorption band at 566 nm observed for the AuNPs 5% tea solution or that at ca. 602 nm for the larger-sized AuNPs 10% tea (57–113 nm, see below) (Figure 1).
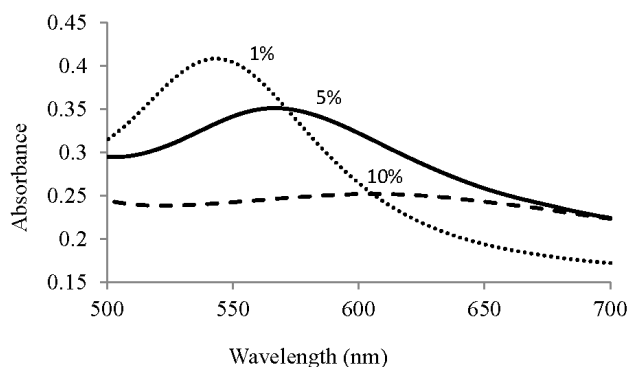
Figure 1. Visible absorbance spectra for AuNPs produced using 1, 5, and 10% tea solutions.

X-ray photoelectron spectroscopy (XPS) exhibits, in the Au 4f region, a single doublet with the Au $4f_{7/2}$ component centered at 84.4 ± 0.3 eV (Figure 2). This doublet shows that AuNPs in the 1% tea extract result from the Au^{3+} reduction to Au^0 and/or Au^+ and that the precursor no longer exists in the solution [45]. It is worth to notice that although the binding energy for bulky Au^0 is established to be centered at 83.95 eV [46], drifts to larger or lower binding energies have been reported for very small gold nanoparticles [47]. Besides Au (0.1%), the surface also shows potassium (1.7%), chlorine (2.6%), nitrogen (2.7%), oxygen (29.4%), and carbonaceous species (63.5%), probably due to the tea extract. It is worth to emphasize that in XPS, the atomic percentage depends on the aggregation state. Therefore, for an element in the form of nanoparticles, the atomic percentage is much lower than what it would be if the component atoms were dispersed on the surface. This explains why the gold percentage is the lowest one.
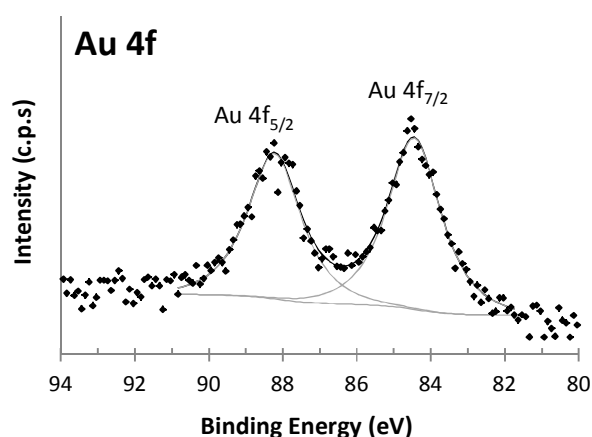
Figure 2. X-ray photoelectron spectroscopy (XPS) Au 4f region for the AuNPs 1% tea.

3.2. Characterization of AuNPs

Transmission electron microscopy (TEM) was used to determine the details of the microstructure in the samples (Figure 3). The AuNPs produced using a 1% (Figure 3a) or a 10% (Figure 3b) tea extract are spherical and dispersed with nearly no aggregations, which was mainly due to the stabilization effect of the tea extract. The size distribution histograms of the AuNPs (Figure 3c,d) were calculated from the corresponding TEM image in Figure 3a,b by measuring the particles in the image; the average particle sizes being in the 8–24 nm and 57–113 nm ranges, respectively.

The analysis of the AuNPs by energy dispersive X-ray spectroscopy (EDS) confirmed the presence of the signals characteristic of gold, demonstrating the successful immobilization of AuNPs (Electronic Supplementary Information, ESI, Figure S2). Figure 4 shows the scanning electron microscopy (SEM) images of typical samples of AuNPs. Moreover, the combination of

SEM and TEM images allows us to conclude that the use of different concentrations of tea extract produced nanoparticles with different sizes. The AuNPs 1% tea are smaller than the AuNPs 10% tea, although both are well dispersed throughout the tea extract. The small white points in Figure 4b are more clear than in Figure 4a due to the diference in the size of AuNPs. For AuNPs 1% tea (Figure 4a), the average size of the AuNPs is smaller than for that of th 10% tea extract. This is in accordance with the size distribution plot produced from the TEM results. The dried tea extract appears as large chunks where the AuNPs are embedded.
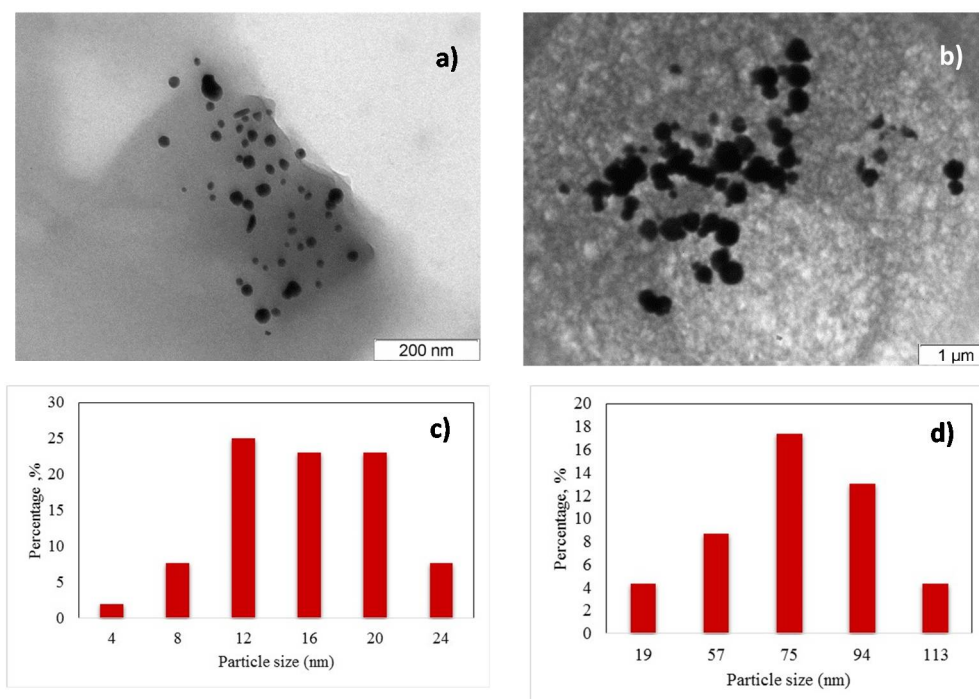
Figure 3. TEM images and size distribution of AuNPs 1% tea (**a**,**c**) and AuNPs 10% tea (**b**,**d**).
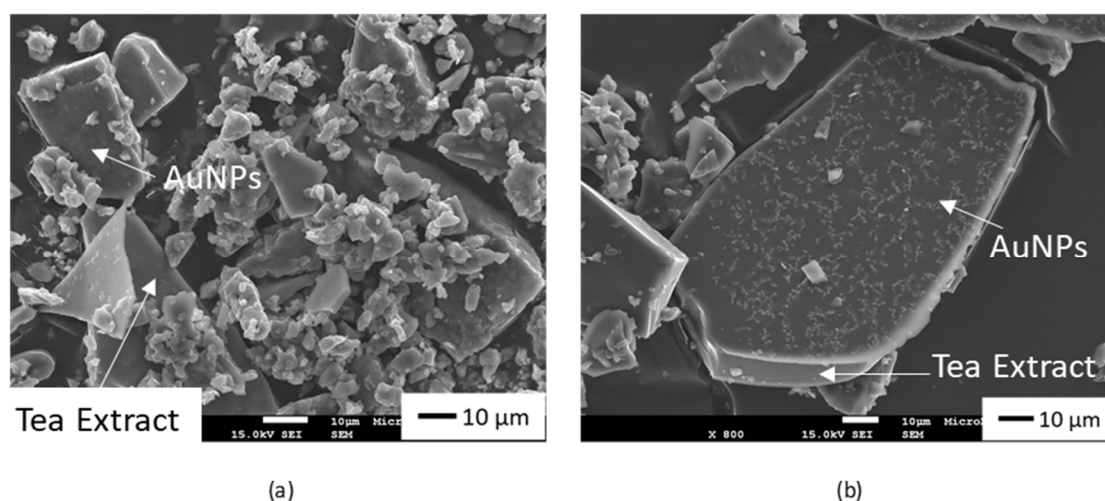
Figure 4. Scanning electron microscopy (SEM) images of (**a**) AuNPs 1% tea and (**b**) AuNPs 10% tea.

FTIR spectra (ESI, Figure S3) were run to identify functional groups on the synthesized AuNPs' surface. They were recorded for the dried tea extract (before reaction with $HAuCl_4 \cdot 3H_2O$) and for the synthetized AuNPs, and showed a great analogy.

Both FTIR spectra displayed a strong and broad signal at 3432 cm^{-1} (hydroxyl group of alcohols or phenols) and a much weaker one at 2926 cm^{-1} (aliphatic CH$_2$ asymmetric stretching). The band at 1700–1637 cm^{-1} is due to ν(C=O) of conjugated ketones, aldehydes, quinines, and esters, whereas that at ca. 1406 cm^{-1} is assigned to the deformation of –CH$_3$ of alkyl groups from the tea constituents. This could be due to the existence of bioactive molecules in the tea in the absence and in the presence of the AuNPs' surface.

3.3. Determination of Total Polyphenol Content

The different tea extracts (1, 5, and 10%) as well as the produced AuNPs solutions (AuNPs 1% tea, AuNPs 5% tea, and AuNPs 10% tea, respectively), before and after the catalytic reduction of 4-nitrophenol, were analyzed for their total polyphenol content (TPC) (Figure 5). The total polyphenol concentration in the prepared tea stock solutions is 1.18 g/L (for 1% *w/v* solution), 3.28 g/L (for 5% *w/v* solution), and 3.55 g/L (for 10% *w/v* solution), respectively, and as expected, proportional to the amount of tea leaves used to prepare those aqueous solutions (Figure 5, entries 1, 4, and 7).

The polyphenol levels present in the tea extract containing the produced AuNPs (0.46, 2.14, and 2.84 g/L for AuNPs 1% tea, AuNPs 5% tea, and AuNPs 10% tea, respectively) was determined and a reduction of 61, 35, and 20% was observed relative to the initial content (Figure 5, entries 2, 5, and 8). As shown, there is a correlation between the percentage of polyphenols consumed and the size of the produced nanoparticles. As the size of the AuNPs decreased, the amount of polyphenol used for their formation increased (Figure 5). After the catalytic reduction of 4-NP in the presence of AuNPs, the resulting solutions were analyzed and a slight decrease of polyphenol amount was detected for the AuNPs 5% and AuNPs 10% solutions (Figure 5, entries 6 and 9 in comparison with entries 5 and 8, respectively).
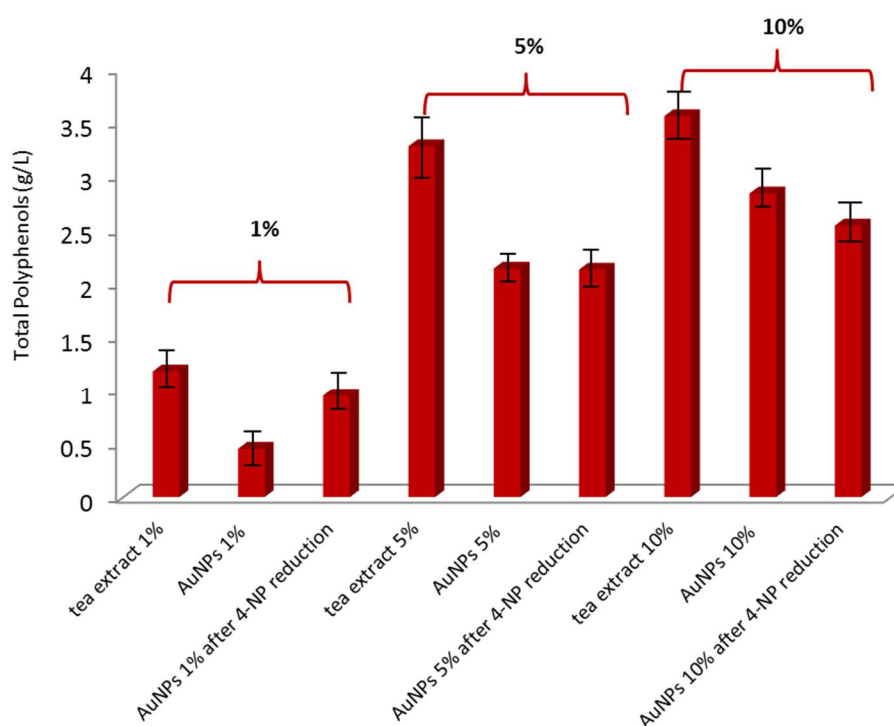
Figure 5. Concentration of total polyphenols in solution (g/L) (4-NP = 4-Nitrophenol).

Surprisingly, for the AuNPs 1% tea solution, an important increase of polyphenols was detected after the catalytic reduction of 4-NP (Figure 5, entry 3 in comparison with entry 2). This fact can be attributed to (i) conceivable regeneration of polyphenols under catalytic reaction conditions and (ii) possible interference of the small AuNPs with the polyphenol measurements [48].

The surface plasmon resonance wavelength of AuNPs is strongly dependent on the size of individual AuNPs. The enhanced surface plasmon resonance effect of AuNPs is a function of the average size and size distribution. The increasing content of polyphenols after the reaction can be attributed to organic compounds present in the extract and not involved in the characteristic Folin–Ciocalteu reaction, resulting in an overestimation.

3.4. Catalytic Studies

The catalytic activity of the prepared AuNPs was investigated for the reduction of various aromatic nitro compounds, namely 2- and 4-nitrophenol (2- and 4-NP); 2-, 3-, and 4-nitroaniline (2-, 3-, and 4-NA); and nitrobenzene (NB) in aqueous medium.

3.4.1. Reduction of 4-Nitrophenol in Aqueous Solution

Catalytic reduction reactions were performed in a standard 3 mL quartz cuvette with a 1 cm path length. The UV–vis absorbance spectra were recorded in the 200–700 nm range at 2 min intervals. A shift of the corresponding absorbance peak at 315 nm to 400 nm occurred immediately after the addition of $NaBH_4$. This new peak (at 400 nm) is attributed [27–32] to the 4-nitrophenolate ion formed in the presence of $NaBH_4$.

The decrease of the intensity of the latter peak readily started in the presence of AuNPs solution and was monitored by UV–vis spectroscopy upon recording the absorbance spectra at 2 min intervals (Figure 6 for 4-NP reduction in the presence of AuNPs 1% tea). The catalytic reduction of 4-nitrophenol (4-NP) to 4-aminophenol (4-AP), widely applied as an industrial chemical and metabolite of common household analgesics such as paracetamol [49], was originally applied by Pal et al. [35] and Esumi et al. [36] to test the catalytic activity of free and immobilized NPs. More recently, this system has been established as a model reaction to evaluate the catalytic performance of different mono- and bimetallic nanoparticles [35,50].
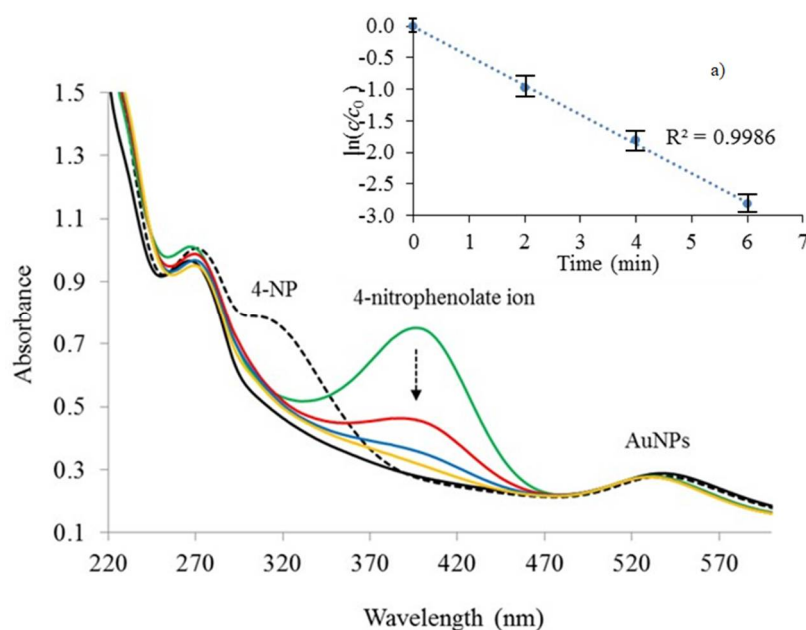
Figure 6. UV–vis spectra over the course of the reduction of 4-nitrophenol (4-NP) by AuNPs 1% tea. Reaction conditions: [AuNPs] = 3.2×10^{-5} M; [4-NP] = 3.8×10^{-5} M; [$NaBH_4$] = 1.6×10^{-3} M. Starting AuNPs tea extract aqueous solution (dark solid line); upon addition of 4-NP (dark dashed line); formation of 4-nitrophenolate (green solid line). Reduction reaction after 2 min (red solid line), after 4 min (blue solid line), and after 6 min (yellow solid line). Inset: a) $\ln(c/c_0)$ versus time (c = [4-nitrophenolate]).

Our study concerned the catalyzed reduction of 4-NP (Scheme 1) in the presence of the synthesized AuNPs, using sodium borohydride (NaBH$_4$) as reducing agent. The three types of AuNPs (1, 5, and 10%) were initially tested, and the best results (see below) were obtained for AuNPs 1% tea. Thus, we chose these AuNPs for further studies. 4-Aminophenol (4-AP) is the only reduction product obtained, and the high selectivity was confirmed [27–32] by UV–vis spectroscopy.

The effect of different reducing agents other than NaBH$_4$ was also studied. Although in the presence of hydrazine, the formation of the intermediate 4-nitrophenolate ion was observed, further reduction to 4-aminophenol was very slight, whereas using other reducing agents such as ascorbic acid, D-glucose, or NH$_4$Cl, even the formation of the intermediate ion was not detected.
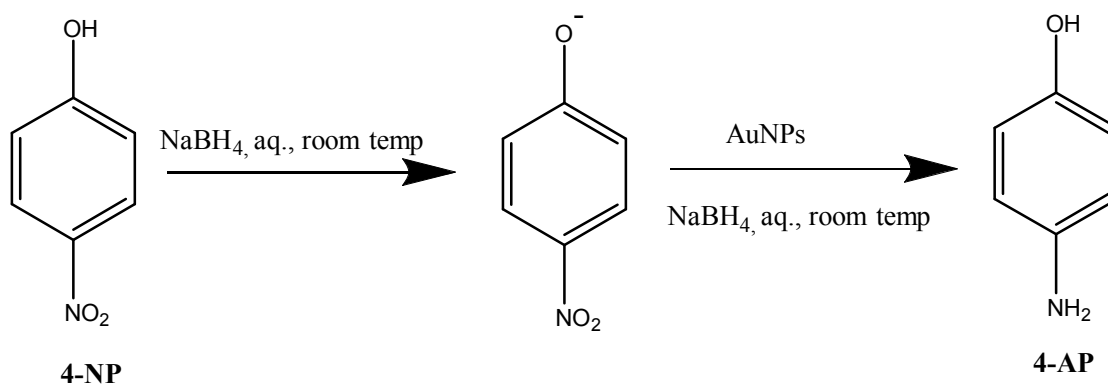
Scheme 1. Reduction of 4-nitrophenol (4-NP) to 4-aminophenol (4-AP) by NaBH$_4$ catalyzed by AuNPs.

In this method, the limitation resides in that the concentration of the 4-nitrophenolate ion, and thus the absorbance at 400 nm, is also dependent on other water chemistry parameters, namely the pH of the solution. The pKa of 4-nitrophenol is 7.2 at room temperature, with the 4-nitrophenolate ion as the dominant species at pH > 7.2. The introduction of the reducing agent (sodium borohydride) into the reaction mixture increases the pH and changes the acid–base speciation of 4-nitrophenol (as Scheme 1 and Figure 6 show). To determine if the tea extract has pH-buffering capacity that may gradually decrease the pH of the reaction mixture over time and thus lead to a lowering of the 4-nitrophenolate ion concentration, we monitored the pH of the reaction mixtures over time under the same conditions, and realized that in the case of the reaction in water, the pH increased in the case of using NaBH$_4$; however, under the same conditions, but without adding NaBH$_4$, the pH of the tea extract solution remains constant (pH $\approx$ 7). There is a slight increase immediately after the addition of NaBH$_4$, but rapidly decreases to the original pH value. From this effect, the decrease in the absorbance at 400 nm is due to the combined effects of the AuNP-catalyzed reduction and changes in pH.

Upon addition of the AuNPs, the electron donor (BH$_4^-$) and electron acceptor (4-nitrophenolate) are both adsorbed on the NP surface and the catalytic reduction of nitrophenolate by BH$_4^-$ starts. In the absence of any catalyst, the formation of the 4-nitrophenolate ion is observed, but no further conversion to 4-aminophenol occurs, and the peak at 400 nm remains unaltered for a long period of time (several days). Thus, AuNPs promote the reduction of 4-nitrophenol by lowering the activation energy of this reaction [51]. In the absence of NaBH$_4$, the AuNPs 1% tea catalyst showed no catalytic activity.

The peak due to 4-aminophenol expected at ca. 290 nm (observed for a pure 4-AP solution) could not be clearly observed in our case, since it is masked underneath the absorption band of the tea extract. This absorption band is due to the presence of polyphenols, confirming the strong UV absorbance of the black tea extract.

The size of metal NPs plays an important role in catalytic systems [52], and thus the application of different sizes of AuNPs in the reduction of 4-nitrophenol was studied (Figure 7). Although the catalytic activity of the AuNPs usually increases when the size of the particles decreases [52–54], an optimal particle size for a particular catalytic system can occur [55,56].

The size of the AuNPs influences the facility with which the substrate (4-NP) and the reducing agent (BH_4^-) are adsorbed on the NP surface. Thus, larger nanoparticles show a lower specific surface area and hinder the approach and adsorption of the reactants, lowering their catalytic performance [51]. For instance, for the larger-sized nanoparticles, that is, 75 nm or AuNPs 10% tea, the conversion of 4-NP achieved after the first 6 min of reaction time is ca. 60%, whereas the smaller AuNPs (AuNPs 1% tea), prepared using the less concentrated tea solution, converts 94% of 4-NP (Figure 7).
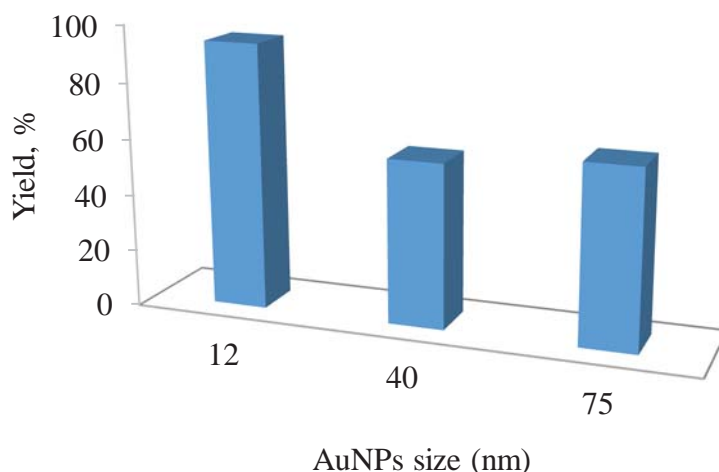
Figure 7. Conversion of 4-nitrophenol (4-NP) to 4-aminophenol (4-AP) as a function of the size of the AuNPs, in the first 6 min of reaction. [AuNPs] = 3.2×10^{-5} M; [4-NP] = 3.8×10^{-5} M; [NaBH$_4$] = 1.6×10^{-3} M.

The effect of catalyst (AuNPs) concentration on the 4-NP reduction reaction was also studied (Table 1, Figure 8 and Figure S4). The conversion is estimated by the decrease of the band at 400 nm, which is characteristic of the 4-nitrophenolate ion.

For a very low concentration (3×10^{-7} M) of AuNPs, almost no conversion of 4-NP to 4-AP was detected after 40 min reaction (entry 1, Table 1). Increasing the catalyst concentration results in a clear rate enhancement. For example, for a 8×10^{-6} M catalyst concentration, a conversion of 72% is observed after 18 min (entry 3, Table 1), whereas for 3.2×10^{-5} M catalyst, a conversion of 94% is achieved after only 6 min (entry 5, Table 1). Blank tests (in the absence of any NP catalyst) were also performed under common reaction conditions, and no conversion was observed.

Since the reducing agent NaBH$_4$ is in a high excess relatively to 4-NP, the reaction is expected to be independent of NaBH$_4$ concentration [33,34] and to follow pseudo first-order kinetics (Equations (1) and (2)), where c and c_0 are the concentrations of 4-nitrophenolate at time t and at $t = 0$, respectively, and $\ln(c/c_0) = \ln(A/A_0)$, where A and A_0 are the corresponding absorbances of the typical band at 400 nm [33,34,57].

$$-\frac{dc}{dt} = k'_{app} \cdot c \tag{1}$$

$$\ln(c/c_0) = -k'_{app} \cdot t \tag{2}$$

The value of k_{app} is the slope of the plot of $\ln(A/A_0)$ versus time (see Figure 6a) for the case of AuNPs 1% tea.

A plot of the apparent rate constant versus the concentration of the catalyst is shown in Figure 8, allowing the rate constant (k) to be obtained as the slope (1.50 ± 0.05 M$^{-1}\cdot$min^{-1}).

Furthermore, since the particle size distribution studies indicated that the NPs formed were nearly uniform in size and spherical in shape, we have used the method adopted by Pikeramenou et al. [58] to calculate the number of particles present (ESI, Table S1) in each amount of composite used for catalysis.

Table 1. Apparent rate constant, conversion, and TOF for the reduction of 4-NP to 4-AP with variable concentrations of AuNPs [a].

Entry	[AuNPs] (M)	$k_{app} \times 10^3$ (min^{-1})	Conversion [b] (%)	TOF [b,c] (h^{-1})	Time [d] (min)	Conversion (%)	TOF [c] (h^{-1})
1	3.0×10^{-7}	0.1	0.0	0.0	40	0.4	5.1
2	2.8×10^{-6}	22.2	0.0	0.0	20	9.3	25.8
3	8.0×10^{-6}	82.8	22.7	72.8	18	72.1	77.1
4	2.3×10^{-5}	325	64.3	71.8	14	93.1	45.2
5	3.2×10^{-5}	464	94.0	75.4	6	94.0	75.4

[a] Reaction conditions: [4-NP] = 3.8×10^{-5} M, [NaBH$_4$] = 1.6×10^{-3} M, catalyst = AuNPs 1% tea. [b] 6 min reaction time. [c] TOF = TON per hour (estimated from Equation (3), see ESI, Table S1); TON = number of moles of product per mol of metal catalyst. [d] Time beyond which no further conversion was significant. k_{app} = apparent rate constant.

This method was applied to calculate the number of surface atoms present in the NPs, which was further used for the calculations of the turnover frequency (TOF) (Equation (3)).

$$TOF = \frac{M}{N_{tS} \cdot t} \tag{3}$$

where M is the number of molecules (4-NP) which reacted in the presence of catalyst in time t to produce the product (4-AP) and N_{tS} is the total number of Au surface atoms of the catalyst that are available for the reaction. The details of the method and calculations are included in the Electronic Supplementary Information, ESI.

As expected, the rate of reduction of nitrophenol increases linearly with the catalyst concentration (Figure 8) [59–61].
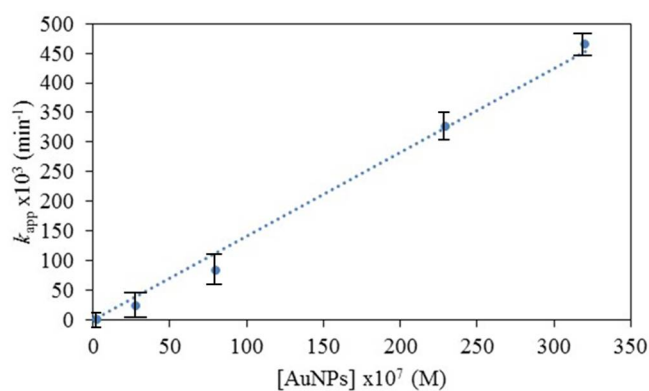
Figure 8. Plot of apparent rate constant k_{app} versus concentration of AuNPs (data from Table 1).

Comparable rates were observed by Panigrahi et al. [39] for the reduction of a series of aromatic nitrocompounds by core-shell nanocomposites (R-Au) bearing, at the surface, well-defined AuNPs of variable sizes (8–55 nm) [39] or by Gangula et al. [57] for the reduction of 4-NP to 4-AP with naturally produced AuNPs (from the stem extract of *Breynia rhamnoides*), although with a larger average size (30 nm), and thus less active, than the AuNPs prepared in our work.

The influence of NaBH$_4$ concentration was also investigated for the reduction of 4-NP, for a constant concentration of AuNPs (Table 2, Figure 9 and Figure S5). For the very low NaBH$_4$ concentration of 4×10^{-5} M, no conversion is observed, even after 40 min of reaction time. Increasing the [NaBH$_4$] to 8×10^{-4} M allows a 30% conversion to be achieved after the same time (entry 3, Table 2), whereas a conversion of 94% is obtained after only 6 min (entry 5, Table 2) for [NaBH$_4$] of 1.6×10^{-3} M. No catalyst poisoning seems to occur, since the characteristic strong UV–vis adsorption band of the AuNPs at ca. 538 nm remains with the same intensity. Calculation of the

apparent rate constant (k'_{app}) is performed assuming that the reaction follows a pseudo-first order law (Equations (4) and (5)), where c and c_0 are the concentrations of 4-nitrophenolate at time t and at $t = 0$, respectively, and $\ln(c/c_0) = \ln(A - A_b/A_0 - A_b)$, where A_0 and A are the absorbances at 400 nm at instant $t = 0$ and t, respectively, and A_b is the background. All the values presented show the correction due to the background absorbance at 400 nm.

$$-\frac{dc}{dt} = k'_{app} \cdot c \tag{4}$$

$$\ln\left(\frac{c}{c_0}\right) = -k'_{app} \cdot t \tag{5}$$

Higher concentrations of NaBH$_4$ for the 4-nitrophenol-catalyzed reduction induce faster kinetics from zero- to first-order kinetics (ESI, Figures S5 and S6).

The rate of reaction also increases with the concentration of sodium borohydride, as observed by other authors [34,39,59].
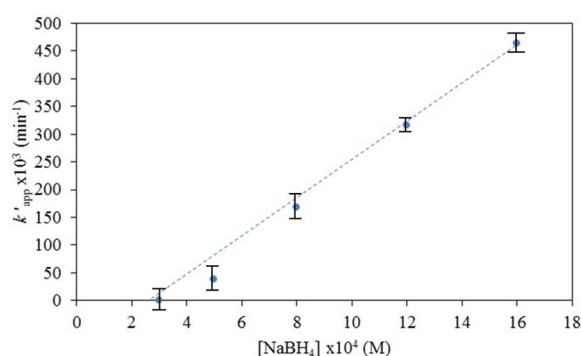
Figure 9. Plot of apparent rate constant k'_{app} obtained from Table 2 versus concentration of NaBH$_4$ (data from Table 2).

Table 2. Reduction of 4-NP to 4-AP with variable concentrations of NaBH$_4$ [a].

Entry	[NaBH$_4$] (M)	$k'_{app} \times 10^3$ (min^{-1})	Conversion [b] (6 min) (%)	Time [d] (min)	Conversion (%)	TOF [c] (h^{-1})
1	3.0×10^{-4}	1.0	0.0	40	2.4	8.5
2	5.0×10^{-4}	38.1	2.4	40	18.5	43.9
3	8.0×10^{-4}	168	22.8	40	30.2	130
4	1.2×10^{-3}	315	55.9	14	88.2	76.3
5	1.6×10^{-3}	464	94.0	6	94.0	127

[a] Reaction conditions: [4-NP] = 3.8×10^{-5} M and [AuNPs 1%] = 3.2×10^{-5} M. [b] 6 min reaction time. [c] TOF = TON per hour (estimated from Equation (3)); TON = number of moles of product per mol of metal catalyst. [d] Time beyond which no further conversion was significant.

3.4.2. Reduction of Other Nitro Compounds

The catalytic activity of the AuNPs 1% was also evaluated for the reduction of 2-nitrophenol (2-NP), nitroanilines (NA), and nitrobenzene (NB), with NaBH$_4$ as the reducing agent (Table 3, Figures S7–S9).

In all cases, the conversion is more efficient for the compounds with the nitro group in the 4-position in comparison with those in the 2- and 3-positions (Table 3). For instance, for the reduction of 4-NA to 4-phenylenediamine (4-PD), 77% conversion is achieved shortly after 8 min (entry 4, Table 3); while for 2- and 3-NA (entries 2 and 3, Table 3), the conversion is 40% and 15%, respectively.

The product of 4-NA reduction, 4-phenylenediamine (4-PD), is an important member of aminobenzenes, with applications in dyes [62] and rubber antioxidants [63], and can also be used as a precursor to aramid textile fibers, thermoplastics, and cast elastomers [64]. In industry,
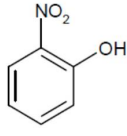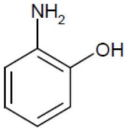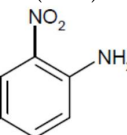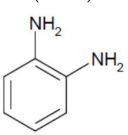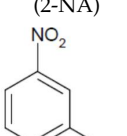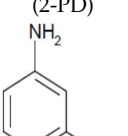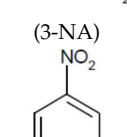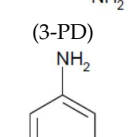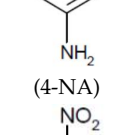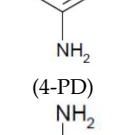
the preparation of 4-PD involves the catalytic hydrogenation of 4-NA [64]. Thus, developing an economic and simple route to its preparation is of great interest.

The intensity decrease of the absorbance peak at 380 nm, due to 4-NA, during the reduction (Figure S8) is accompanied by the appearance of a new one at 308 nm, corresponding to the formation of 4-PD. Another characteristic peak of 4-PD at 238 nm is not visible due to the overlap with a tea extract absorption band. Initially, no other products were detected, but after a longer period of reaction, reoxidation of the amino group of 4-PD to give benzoquinone and/or azobenzene may occur (with appearance of a new absorption band at ca. 486 nm) [65].

The reduction of nitrobenzene (NB), since the classical work by Haber [66], is a well-studied reaction. In the presence of AuNPs, the reduction proceeds only along the so-called direct route, via nitrosobenzene and phenylhydroxylamine [67–69].

In our catalytic system, nitrobenzene is less reactive than 4-NP against $NaBH_4$ in the presence of the same amount of AuNPs (3.2×10^{-5} M), and provides, after 8 and 14 min (ESI, Figure S9), ca. 61% (entry 5, Table 3) and 70% conversion, respectively. After 40 min, the conversion is not yet complete.

Table 3. Reduction of various substrates using AuNPs 1% tea as catalyst [a].

Entry	Substrate	Product	$k_{app} \times 10^2$ (min^{-1})	Time (min)	Conversion (%)	TOF [b] (h^{-1})
1	(2-NP)	(2-AP)	23.9	8	80	61.1
2	(2-NA)	(2-PD)	17.3	8	40	30.5
3	(3-NA)	(3-PD)	2.5	8	15	11.4
4	(4-NA)	(4-PD)	37.8	8	77	58.7
5	(NB)	(NA)	4.6	8	61	46.5

[a] Reaction conditions: [AuNPs 1%] = 3.2×10^{-5} M; [substrate] = 3.8×10^{-5} M; [$NaBH_4$] = 1.6×10^{-3} M at 25 °C.
[b] TOF = TON per hour; TON = number of moles of product per mol of metal catalyst.

3.4.3. Recycling Studies for AuNPs in 4-NP Reduction

To check the possibility of reutilization and recycling of our AuNPs as the catalyst in the reduction of nitro compounds, we repeated the reduction experiments of 4-NP via two different procedures

(I and II). In the first one (I), 4-NP reduction was performed through sequential addition of new portions of substrate (after the previous one had been consumed) to an aqueous solution containing NaBH$_4$ in excess and AuNPs 1% tea (Figure 10). The AuNPs become less efficient upon each new addition of 4-NP. However, even after the third addition of substrate (Figure 10c) and in the presence of the initial AuNPs catalyst, conversion of 4-NP to 4-AP is still observed, although taking longer to almost complete the transformation (26 min in comparison with the 10 min of the second addition (Figure 10b) or the 2 min for the first one (Figure 10a)).

After the fourth addition of substrate (Figure 10d), it was found that the conversion stagnated after 12 min. However, upon addition of a new amount of the reducing agent NaBH$_4$, a full descent of the characteristic band of the 4-nitrophenolate was detected, demonstrating the complete conversion of the substrate and that the AuNPs 1% are still active and therefore available for recycling.

The recycling of the AuNPs 1% catalyst was also studied (procedure II), by separating the AuNPs from the reaction mixture (by centrifugation) after a first reduction reaction (Figure 10a).

The deposited AuNPs were washed with distilled water, and new portions of 4-NP and reducing agent were added (Figure 11). The volume was completed with distilled water.

The reduction of 4-NP takes 32 min to be completed, whereas in the first method, it happens after 10 min (Figure 10b). It was also found that since the tea solution was removed after centrifugation, the characteristic band of 4-AP at 290 nm is now visible and not masked with tea extract bands. Moreover, the tendency to form agglomerates using the last method could lead to the reduced reactivity and stability of these nanoparticles [70]. In fact, in the first cycles, a shift from 538 nm to 630 nm in the characteristic band of AuNPs was observed, indicating that the size of the nanoparticles increased due to aggregation. With the progression of the reaction, a new shift in the band, now to lower wavelengths, is observed. The change could be due to the reaction of the reducing agent with AuNPs, promoting their decrease in size.
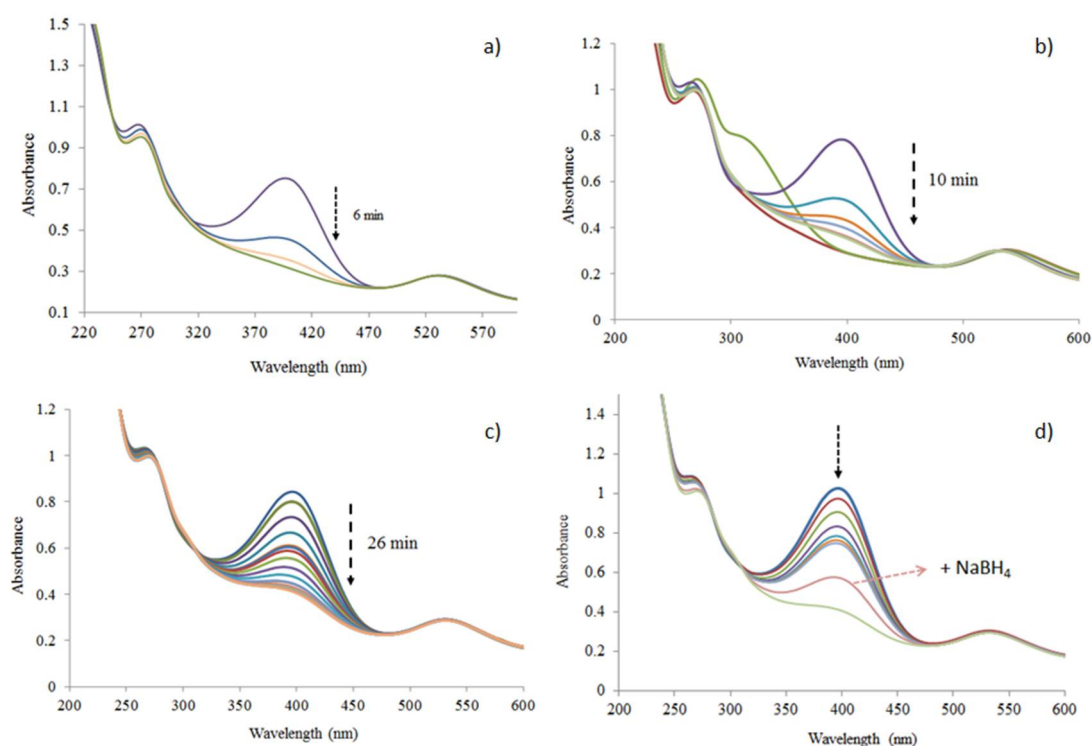
Figure 10. Reutilization of AuNPs 1% tea as the catalyst in the reduction of 4-NP. (**a**) First addition of 4-NP; (**b**) second addition of 4-NP; (**c**) third addition of 4-NP; (**d**) fourth addition of 4-NP and subsequent addition of NaBH$_4$. All additions were in identical conditions to those of entry 5, Table 1.

The heterogeneous nature of the catalytic process was also proven as follows. After the first cycle, the AuNPs were separated from the final reaction mixture by centrifugation (Figure 11). The resulting solution was also tested for the reduction of 4-NP, and no activity was observed. Moreover, the AuNP characteristic absorption band was not detected.

The use of a heterogeneous nanocatalyst produced by an eco-friendly procedure is still an underdeveloped field, and a comparison with other related cases shows that our catalyst is more active than a similar one supported in multiwalled carbon nanotubes [71], where the reduction of 4-NP was not complete even after 2 h. In the case of the AuNPs synthesized from the stem extract of *Breynia rhamnoides* [57], 90% conversion was observed after 7 min, whereas over 94% conversion was observed in 6 min with the AuNPs 1% tea produced in this work.
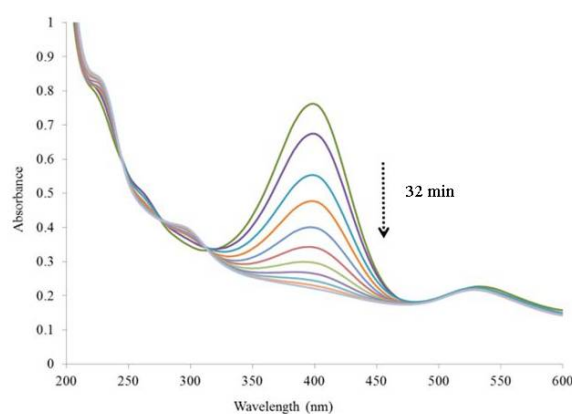
Figure 11. Recycling of AuNPs 1% tea (separated by centrifugation) as the catalyst in the reduction of 4-NP.

4. Conclusions

The results show that AuNPs were successfully synthesized in a single step process upon reduction of $HAuCl_4 \cdot 3H_2O$ by polyphenols and flavonoids present in black tea, without using a surfactant. These gold nanoparticles were utilized as efficient heterogeneous catalysts for the reduction of nitro compounds. High conversions into the corresponding amino-products were obtained, no particle aggregation occurred during the catalytic process, and the AuNP catalyst can be easily reused and recycled. The black tea method used for the synthesis of nanoparticles is quite simple and environmentally benign, and the work shows that the AuNPs obtained thusly act as good catalysts for nitro reductions, thus promoting greener and safer methodologies for such reactions.

Conflicts of Interest: The authors declare no conflict of interest.

References

1. Iravani, S.; Korbekandi, H.; Mirmohammadi, S.V.; Zolfaghari, B. Synthesis of silver nanoparticles: Chemical, physical and biological methods. *Res. Pharm. Sci.* **2014**, *9*, 385–406. [PubMed]

2. Iravani, S. Green synthesis of metal nanoparticles using plants. *Green Chem.* **2011**, *13*, 2638–2650. [CrossRef]

3. He, S.; Guo, Z.; Zhang, Y.; Zhang, S.; Gu, J.W. Biosynthesis of gold nanoparticles using the bacteria *Rhodopseudomonas capsulate*. *Mater. Lett.* **2007**, *61*, 3984–3987. [CrossRef]

4. Southam, G.; Beveridge, T.J. The occurrence of bacterially derived sulphur and phosphorus within pseudocrystalline and crystalline octahedral gold formed in vitro. *Geochim. Cosmochim. Acta* **1996**, *60*, 4369–4376. [CrossRef]

5. Ahmad, A.; Mukherjee, P.; Senapati, S.; Mandal, D.; Khan, M.I.; Kumar, R.; Sastry, M. Extracellular biosynthesis of silver nanoparticles using the fungus *Fusarium oxysporum*. *Colloids Surf. B* **2003**, *28*, 313–318. [CrossRef]

6. Ankamwar, B. Biosynthesis of Gold Nanoparticles (Green-gold) Using Leaf Extract of *Terminalia catappa*. *J. Chem.* **2010**, *7*, 1334–1339.

7. Huang, L.; Weng, X.; Chen, Z.; Megharaj, M.; Naidu, R. Green synthesis of iron nanoparticles by various tea extracts: Comparative study of the reactivity. *Spectrochim. Acta A* **2014**, *130*, 295–301. [CrossRef] [PubMed]

8. Santos, S.A.O.; Pinto, R.J.B.; Rocha, S.M.; Marques, P.A.A.P.; Neto, C.P.; Silvestre, A.J.D.; Freire, C.S.R. Unveiling the chemistry behind the green synthesis of metal nanoparticles. *ChemSusChem* **2014**, *7*, 2704–2711. [CrossRef] [PubMed]

9. Kharissova, O.V.; Dias, H.V.R.; Kharisov, B.I.; Pérez, B.O.; Pérez, V.M.J. The greener synthesis of nanoparticles. *Trends Biotechnol.* **2013**, *31*, 240–248. [CrossRef] [PubMed]

10. Nadagouda, M.N.; Varma, R.S. Green synthesis of silver and palladium nanoparticles at room temperature using coffee and tea extract. *Green Chem.* **2008**, *10*, 859–862. [CrossRef]

11. Huang, J.; Li, Q.; Sun, D.; Lu, Y.; Su, Y.; Yang, X.; Wang, H.; Wang, Y.; Shao, W.; He, N.; et al. Biosynthesis of Silver and Gold Nanoparticles by Novel Sundried *Cinnamomum camphora* Leaves. *Nanotechnology* **2007**, *18*, 105104–105115. [CrossRef]

12. Vilchis-Nestor, A.R.; Sánchez-Mendieta, V.; Camacho-López, M.A.; Gómez-Espinosa, R.M.; Camacho-López, M.A.; Arenas-Alatorre, J.A. Solventless synthesis and optical properties of Au and Ag nanoparticles using *Camellia sinensis* extract. *Mater. Lett.* **2008**, *62*, 3103–3105. [CrossRef]

13. Moreno-Mañas, M.; Pleixats, R. Formation of Carbon–Carbon Bonds under Catalysis by Transition-Metal Nanoparticles. *Acc. Chem. Res.* **2003**, *36*, 638–643. [CrossRef] [PubMed]

14. Ren, X.; Meng, X.; Chen, D.; Tang, F.; Jiao, J. Using silver nanoparticle to enhance current response of biosensor. *Biosens. Bioelectron.* **2005**, *21*, 433–437. [CrossRef] [PubMed]

15. Dhayalan, M.; Denison, M.I.J.; Jegadeeshwari, A.; Krishnan, K.; Gandhi, N. In vitro antioxidant, antimicrobial, cytotoxic potential of gold and silver nanoparticles prepared using *Embelia ribes*. *Nat. Prod. Res.* **2017**, *31*, 456–468. [CrossRef] [PubMed]

16. Sharma, R.K.; Gulati, S.; Mehta, S. Preparation of Gold Nanoparticles Using Tea: A Green Chemistry Experiment. *J. Chem. Educ.* **2012**, *89*, 1316–1318. [CrossRef]

17. Daniel, M.C.; Astruc, D. Gold Nanoparticles: Assembly, Supramolecular Chemistry, Quantum-Size-Related Properties, and Applications toward Biology, Catalysis, and Nanotechnology. *Chem. Rev.* **2004**, *104*, 293–346. [CrossRef] [PubMed]

18. Dykmana, L.; Khlebtsov, N. Gold nanoparticles in biomedical applications: Recent advances and perspectives. *Chem. Soc. Rev.* **2012**, *41*, 2256–2282. [CrossRef] [PubMed]

19. Rodriguez-Lorenzo, L.; Rica, R.; Alvarez-Puebla, R.A.; Liz-Marzan, L.M.; Stevens, M.M. Plasmonic nanosensors with inverse sensitivity by means of enzyme-guided crystal growth. *Nat. Mater.* **2012**, *11*, 604–607. [CrossRef] [PubMed]

20. Thielecke, N.; Aytemir, M.; Pruesse, U. Selective oxidation of carbohydrates with gold catalysts: Continuous-flow reactor system for glucose oxidation. *Catal. Today* **2007**, *121*, 115–120. [CrossRef]

21. Han, J.; Liu, Y.; Guo, R. Reactive Template Method to Synthesize Gold Nanoparticles with Controllable Size and Morphology Supported on Shells of Polymer Hollow Microspheres and Their Application for Aerobic Alcohol Oxidation in Water. *Adv. Funct. Mater.* **2009**, *19*, 1112–1117. [CrossRef]

22. Nalawade, P.; Mukherjee, T.; Kapoor, S. Green Synthesis of Gold Nanoparticles Using Glycerol as a Reducing Agent. *Adv. Nanoparticles* **2013**, *2*, 78–86. [CrossRef]

23. Haruta, M. When Gold Is Not Noble: Catalysis by Nanoparticles. *Chem. Rec.* **2003**, *3*, 75–87. [CrossRef] [PubMed]

24. Kumar, A.; Vemula, P.K.; Ajayan, P.M.; John, G. Silver-nanoparticle-embedded antimicrobial paints based on vegetable oil. *Nat. Mater.* **2008**, *7*, 236–241. [CrossRef] [PubMed]

25. Santos, K.O.; Elias, W.C.; Signori, A.M.; Giacomelli, F.C.; Yang, H.J.; Domingos, B. Synthesis and Catalytic Properties of Silver Nanoparticle-Linear Polyethylene Imine Colloidal Systems. *J. Phys. Chem. C* **2012**, *116*, 4594–4604. [CrossRef]

26. Baruah, B.; Gabriel, G.J.; Akbashev, M.J.; Booher, M.E. Facile synthesis of silver nanoparticles stabilized by cationic polynorbornenes and their catalytic activity in 4-nitrophenol reduction. *Langmuir* **2013**, *29*, 4225–4234. [CrossRef] [PubMed]

27. Hayakawa, K.; Yoshimura, T.; Esumi, K. Preparation of Gold-Dendrimer Nanocomposites by Laser Irradiation and Their Catalytic Reduction of 4-Nitrophenol. *Langmuir* **2003**, *19*, 5517–5521. [CrossRef]

28. Kuroda, K.; Ishida, M.; Haruta, M. Reduction of 4-nitrophenol to 4-aminophenol over Au nanoparticles deposited on PMMA. *J. Mol. Catal. A Chem.* **2009**, *298*, 7–11. [CrossRef]

29. Cui, Q.; Yashchenok, A.; Li, L.; Möhwald, H.; Bargheer, M. Mechanistic study on reduction reaction of nitro compounds catalyzed by gold nanoparticles using in situ SERS monitoring. *Colloids Surf. A.* **2015**, *470*, 108–113. [CrossRef]

30. Shah, D.; Kaur, H. Resin-trapped gold nanoparticles: An efficient catalyst for reduction of nitro compounds and Suzuki-Miyaura coupling. *J. Mol. Catal. A* **2014**, *381*, 70–76. [CrossRef]

31. Gu, S.; Wunder, S.; Lu, Y.; Ballauff, M. Kinetic analysis of the catalytic reduction of 4-nitrophenol by metallic nanoparticles. *J. Phys. Chem. C* **2014**, *118*, 18618–18625. [CrossRef]

32. Pradhan, N.; Pal, A.; Pal, T. Catalytic Reduction of Aromatic Nitro Compounds by Coinage Metal Nanoparticles. *Langmuir* **2001**, *17*, 1800–1802. [CrossRef]

33. Johnson, J.A.; Makis, J.J.; Marvin, K.A.; Rodenbusch, S.E.; Stevenson, K.J. Size-Dependent Hydrogenation of *p*-Nitrophenol with Pd Nanoparticles Synthesized with Poly(amido)amine Dendrimer Templates. *J. Phys. Chem. C* **2013**, *117*, 22644–22651. [CrossRef]

34. Hervés, P.; Peréz-Lorenzo, M.; Liz-Marzán, L.M.; Dzubiella, J.; Lu, Y.; Ballauff, M. Catalysis by metallic nanoparticles in aqueous solution: Model reactions. *Chem. Soc. Rev.* **2012**, *41*, 5577–5587. [CrossRef] [PubMed]

35. Pradhan, N.; Pal, A.; Pal, T. Silver nanoparticle catalyzed reduction of aromatic nitro compounds. *Colloid Surf. A Physicochem. Eng. Asp.* **2002**, *196*, 247–257. [CrossRef]

36. Esumi, K.; Isono, R.; Yoshimura, T. Preparation of PAMAM- and PPI-Metal (Silver, Platinum, and Palladium) Nanocomposites and Their Catalytic Activities for Reduction of 4-Nitrophenol. *Langmuir* **2004**, *20*, 237–243. [CrossRef] [PubMed]

37. Errokh, A.; Ferraria, A.M.; Conceição, D.S.; Vieira Ferreira, L.F.; Botelho do Rego, A.M.; Rei Vilar, M.; Boufi, S. Controlled growth of Cu_2O nanoparticles bound to cotton fibres. *Carbohydr. Polym.* **2016**, *141*, 229–237. [CrossRef] [PubMed]

38. Fenger, R.; Fertitta, E.; Kirmse, H.; Thünemann, A.F.; Rademann, K. Size dependent catalysis with CTAB-stabilized gold nanoparticles. *Phys. Chem. Chem. Phys.* **2012**, *14*, 9343–9349. [CrossRef] [PubMed]

39. Panigrahi, S.; Basu, S.; Praharaj, S.; Pande, S.; Jana, S.; Pal, A.; Ghosh, S.K.; Pal, T. Synthesis and Size-Selective Catalysis by Supported Gold Nanoparticles: Study on Heterogeneous and Homogeneous Catalytic Process. *J. Phys. Chem. C* **2007**, *111*, 4596–4605. [CrossRef]

40. Babu, P.J.; Sharma, P.; Saranya, S.; Tamuli, R.; Bora, U. Green Synthesis and Characterization of Biocompatible Gold Nanoparticles Using *Solanum indicum* Fruits. *Nanomater. Nanotechnol.* **2013**, *3*, 4. [CrossRef]

41. Singleton, V.L.; Orthofer, R.; Lamuela-Raventós, R.M. Analysis of total phenols and other oxidation substrates and antioxidants by means of folin-ciocalteu reagent. *Method Enzymol.* **1999**, *299*, 152–178.

42. Link, S.; El-Sayed, M.A. Size and Temperature Dependence of the Plasmon Absorption of Colloidal Gold Nanoparticles. *J. Phys. Chem. B* **1999**, *103*, 4212–4217. [CrossRef]

43. Sareen, S.; Mutreja, V.; Pal, B.; Singh, S. Homogeneous dispersion of Au nanoparticles into mesoporous SBA-15 exhibiting improved catalytic activity for nitroaromatic reduction. *Microporous Mesoporous Mater.* **2015**, *202*, 219–225. [CrossRef]

44. Gu, J.; Fan, W.; Shimojima, A.; Okubo, T. Microwave-induced synthesis of highly dispersed gold nanoparticles within the pore channels of mesoporous silica. *J. Solid State Chem.* **2008**, *181*, 957–963. [CrossRef]

45. Carapeto, A.P.; Ferraria, A.M.; Boufi, S.; Rei Vilar, M.; Botelho do Rego, A.M. Ion reduction in metallic nanoparticles nucleation and growth on cellulose films: Does substrate play a role? *Cellulose* **2015**, *22*, 173–186. [CrossRef]

46. Seah, M.P. Summary of ISO/TC 201 Standard: VII ISO 15472: 2001—Surface chemical analysis—X-ray photoelectron spectrometers—Calibration of energy scales. *Surf. Interface Anal.* **2001**, *31*, 721–723. [CrossRef]

47. Boufi, S.; Ferraria, A.M.; Botelho do Rego, A.M.; Battaglini, N.; Herbst, F.; Rei Vilar, M. Surface functionalisation of cellulose with noble metals nanoparticles through a selective nucleation. *Carbohydr. Polym.* **2011**, *86*, 1586–1594. [CrossRef]

48. Mystrioti, C.; Xanthopoulou, T.D.; Tsakiridis, P.E.; Papassiopi, N.; Xenidis, A. Comparative evaluation of five plant extracts and juices for nanoiron synthesis and application for hexavalent chromium reduction. *Sci. Total Environ.* **2016**, *539*, 105–113. [CrossRef] [PubMed]

49. Çekiç, S.D.; Filik, H.; Apak, R. Simultaneous Spectrophotometric Determination of Paracetamol and *p*-Aminophenol in Pharmaceutical Products with Tiron Using Dissolved Oxygen as Oxidant. *J. Anal. Chem.* **2005**, *60*, 1019–1023. [CrossRef]

50. König, R.Y.G.; Schwarze, M.; Schomäcker, R.; Stubenrauch, C. Catalytic Activity of Mono- and Bi-Metallic Nanoparticles Synthesized via Microemulsions. *Catalysts* **2014**, *4*, 256–275. [CrossRef]

51. Antonels, N.A.; Meijboom, R. Preparation of well-defined dendrimer encapsulated ruthenium nanoparticles and their evaluation in the reduction of 4-nitrophenol according to the Langmuir-Hinshelwood approach. *Langmuir* **2013**, *29*, 13433–13442. [CrossRef] [PubMed]

52. Lin, C.; Tao, K.; Hua, D.; Ma, Z.; Zhou, S. Size Effect of Gold Nanoparticles in Catalytic Reduction of *p*-Nitrophenol with NaBH$_4$. *Molecules* **2013**, *18*, 12609–12620. [CrossRef] [PubMed]

53. Shekhar, M.; Wang, J.; Lee, W.-S.; Williams, W.D.; Kim, S.M.; Stach, E.A.; Miller, J.T.; Delgass, W.N.; Riberio, F.H. Size and support effects for the water-gas shift catalysis over gold nanoparticles supported on model Al$_2$O$_3$ and TiO$_2$. *J. Am. Chem. Soc.* **2012**, *134*, 4700–4708. [CrossRef] [PubMed]

54. Shimizu, K.; Miyamoto, Y.; Kawasaki, T.; Tanji, T.; Tai, Y.; Satsuma, A. Chemoselective Hydrogenation of Nitroaromatics by Supported Gold Catalysts: Mechanistic Reasons of Size- and Support-Dependent Activity and Selectivity. *J. Phys. Chem. C* **2009**, *113*, 17803–17810. [CrossRef]

55. Valden, M.; Pak, S.; Lai, X.; Goodman, D.W. Structure sensitivity of CO oxidation over model Au/TiO$_{22}$ catalysts. *Catal. Lett.* **1998**, *56*, 7–10. [CrossRef]

56. Laoufi, I.; Saint-Lager, M.-C.; Lazzari, R.; Jupille, J.; Robach, O.; Garaudée, S.; Cabailh, G.; Dolle, P.; Cruguel, H.; Bailly, A. Size and Catalytic Activity of Supported Gold Nanoparticles: An in Operando Study during CO Oxidation. *J. Phys. Chem. C* **2011**, *115*, 4673–4679. [CrossRef]

57. Gangula, A.; Podila, R.; Ramakrishna, M.; Karanam, L.; Janardhana, C.; Rao, A.M. Catalytic reduction of 4-nitrophenol using biogenic gold and silver nanoparticles derived from *Breynia rhamnoides*. *Langmuir* **2011**, *27*, 15268–15274. [CrossRef] [PubMed]

58. Lewis, J.D.; Day, M.T.; MacPherson, V.J.; Pikramenou, Z. Luminescent nanobeads: Attachment of surface reactive Eu(III) complexes to gold nanoparticles. *Chem. Commun.* **2006**, *17*, 1433–1435. [CrossRef] [PubMed]

59. Spiro, M. Heterogeneous Catalysis of Solution Reactions. In *Essays in Chemistry*; Bradley, J.N., Gillard, R.D., Hudson, R.F., Eds.; Academic Press: London, UK, 1973; Volume 5, p. 63.

60. Gallezot, P.; Laurain, N.; Isnard, P. Catalytic wet-air oxidation of carboxylic acids on carbon-supported platinum catalysts. *Appl. Catal. B* **1996**, *9*, L11–L17. [CrossRef]

61. Pintar, A.; Levec, J. Catalytic oxidation of aqueous *p*-chlorophenol and *p*-nitrophenol solutions. *Chem. Eng. Sci.* **1994**, *49*, 4391–4407. [CrossRef]

62. Clausen, T.; Schwan-Jonczyk, A.; Lang, G.; Schuh, W.; Liebscher, K.D.; Springob, C.; Franzke, M.; Balzer, W.; Imhoff, S.; Maresch, G.; et al. *Hair Preparations*; John Wiley & Sons: New York, NY, USA, 2006.

63. Engels, H.; Weidenhaupt, H.; Pieroth, M.; Hofmann, W.; Menting, K.; Mergenhagen, T.; Schmoll, R.; Uhrlandt, S. *Chemicals and Additives*; John Wiley & Sons: New York, NY, USA, 2004.

64. Smiley, R.A. *Phenylene- and Toluenediamines*; John Wiley & Sons: New York, NY, USA, 2000.

65. Wu, W.; Liang, S.; Chen, Y.; Shen, L.; Zheng, H.; Wu, L. High efficient photocatalytic reduction of 4-nitroaniline to *p*-phenylenediamine over microcrystalline $SrBi_2Nb_2O_9$. *Catal. Commun.* **2012**, *17*, 39–42. [CrossRef]

66. Haber, F.Z. Gradual electrolytic reduction of nitrobenzene with limited cathode potential. *Elektrochem. Angew. Phys. Chem.* **1898**, *22*, 506–514.

67. Corma, A.; Concepcion, P.; Serna, P. A Different Reaction Pathway for the Reduction of Aromatic Nitro Compounds on Gold Catalysts. *Angew. Chem.* **2007**, *119*, 7404–7407. [CrossRef]

68. Corma, A.; Serna, A. Chemoselective hydrogenation of nitro compounds with supported gold catalysts. *Science* **2006**, *313*, 332–334. [CrossRef] [PubMed]

69. Wunder, S.; Polzer, F.; Lu, Y.; Mei, Y.; Ballauff, M. Kinetic Analysis of Catalytic Reduction of 4-Nitrophenol by Metallic Nanoparticles Immobilized in Spherical Polyelectrolyte Brushes. *J. Phys. Chem. C* **2010**, *114*, 8814–8820. [CrossRef]

70. O'Carroll, D.; Sleep, B.; Krol, M.; Boparai, H.; Kocur, C. Nanoscale zero valent iron and bimetallic particles for contaminated site remediation. *Adv. Water Resour.* **2013**, *51*, 104–122. [CrossRef]

71. Abdel-Fattah, T.A.; Wixtrom, A. Catalytic Reduction of 4-Nitrophenol Using Gold Nanoparticles Supported on Carbon Nanotubes. *ECS J. Solid State Sci.* **2014**, *3*, M18–M20. [CrossRef]